

RSC Advances



This is an *Accepted Manuscript*, which has been through the Royal Society of Chemistry peer review process and has been accepted for publication.

Accepted Manuscripts are published online shortly after acceptance, before technical editing, formatting and proof reading. Using this free service, authors can make their results available to the community, in citable form, before we publish the edited article. This *Accepted Manuscript* will be replaced by the edited, formatted and paginated article as soon as this is available.

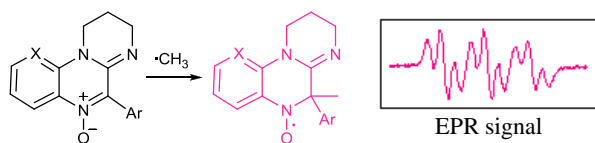
You can find more information about *Accepted Manuscripts* in the [Information for Authors](#).

Please note that technical editing may introduce minor changes to the text and/or graphics, which may alter content. The journal's standard [Terms & Conditions](#) and the [Ethical guidelines](#) still apply. In no event shall the Royal Society of Chemistry be held responsible for any errors or omissions in this *Accepted Manuscript* or any consequences arising from the use of any information it contains.

Amidinoquinoxaline *N*-oxides as novel spin traps

Nadia Gruber, Lidia L. Piehl, Emilio Rubin de Celis, Jimena E. Díaz, María B. García, Pierluigi Stipa, and Liliana R. Orelli

A series of nitrones were synthesized and tested as novel spin traps. The adducts generated by $\cdot\text{CH}_3$ addition showed remarkably persistent signals. Their EPR features and kinetics were rationalised by DFT and MP2 calculations.



Amidinoquinoxaline *N*-oxides as novel spin traps

Cite this: DOI: 10.1039/x0xx00000x

Nadia Gruber,^{a,b,c} Lidia L. Piehl,^b Emilio Rubin de Celis,^b Jimena E. Díaz,^a María B. García,^a Pierluigi Stipa,^{*c} and Liliana R. Orelli^{*a}

Received 00th January 2012,

Accepted 00th January 2012

DOI: 10.1039/x0xx00000x

www.rsc.org/

A novel type of spin traps **1** derived from the pyrimidoquinoxaline *N*-oxide heterocyclic core is reported. EPR technique was used to evaluate their ability to trap methyl radicals generated in a Fenton reaction in the presence of DMSO. All the synthesized nitrones showed spin trapping properties and the corresponding nitroxides **2** were characterized by EPR. The novel spin traps showed remarkably persistent signals, as evidenced in a competition experiment with DMPO. The addition rate constants leading to the spin adducts (k_{add}) were determined, and very good correlations were found with steric and electronic parameters of the parent nitrones. The spin adducts decomposition rate constants (k_{dec}) and the corresponding half-life times ($t_{1/2}$) were also determined. DFT and MP2 calculations were used in order to rationalize the adducts hfcc and the structural factors influencing their addition and decomposition rates.

Introduction

Electron paramagnetic resonance (EPR) spin trapping represents one of the most specific and reliable techniques for detecting and identifying transient free radicals, such as those produced in chemical and biological processes, whose lifetime is too short in the EPR spectroscopic time scale. This technique, widely used since its introduction about 40 years ago,¹ is based upon the fast reaction between a suitable diamagnetic molecule (a spin trap) and short-lived free radicals with formation of relatively long lived radicals (spin adducts), whose EPR signals are persistent enough to be recorded and analyzed. Spectral parameters such as hyperfine coupling constants (hfcc) and *g*-factors are generally characteristic of the type of radical initially trapped. This technique has been successfully used in biological systems, with many applications in a series of human diseases like ischemia-reperfusion syndrome, Friedreich's ataxia, atherosclerosis,² neurodegenerative diseases³ and cellular aging.⁴ Nitrones (*N*-oxides) are very efficient spin traps,⁵ being able to undergo fast radical additions by C- and O-centered radicals, to yield aminoxyls (nitroxides) as spin adducts, these species being among the most persistent organic free radicals in liquid solution. Among the commercially available nitrones, *N*-*tert*-butylbenzylideneamine *N*-oxide (PBN), 5,5-dimethyl-3,4-dihydro-2*H*-pyrrole *N*-oxide (DMPO)⁶ are the most popular, but their use is not without limitations. For example, PBN and its analogues give spin adducts with similar EPR spectra generally consisting of a triplet of doublets with a relatively small variation in the doublet splitting depending on the radical trapped, and this may be a source of misinterpretations in spin trapping experiments.⁷ On the other hand, the use of DMPO is

limited by its sensitivity to nucleophilic attack by water and the relatively low stability of its superoxide spin adduct, which decomposes rapidly.⁸ A continuous effort has been devoted to the synthesis of PBN and DMPO analogues⁹ and of other nitrones¹⁰ to be used in spin trapping experiments without the above mentioned drawbacks. To this end, we synthesized a series of 5-aryl-2,3-dihydro-1*H*-pyrimido[1,2-*a*]quinoxaline 6-oxides **1a-h** and a fused pyridyl analogue **1i** and evaluated their spin trapping ability by EPR spectroscopy. 2,3-Dihydro-1*H*-pyrimido[1,2-*a*]quinoxaline *N*-oxides represent a heterocyclic core of interest due to its pharmacological properties. Some suitably substituted derivatives possess antineoplastic activity,¹¹ especially against hypoxic tumours. Other pyrimidoquinoxaline 6-oxides have been employed as antiamoebic¹² and antianaerobic agents¹³. As part of our research on nitrogen heterocycles, we reported a novel methodology for their synthesis,¹⁴ and investigated some of their chemical,¹⁵ spectroscopic¹⁶ and pharmacological¹⁷ properties.

Two structural features of these compounds which could both have a stabilizing effect on the corresponding spin adducts prompted us to test these nitrones as potential spin traps: the absence of hydrogens α - to the *N*-oxide function and the presence of a conjugated amidine moiety. In fact, it is known that aminoxyls bearing α -hydrogens are unstable and may disproportionate to the corresponding nitrone and a hydroxylamine,¹⁸ while it has been observed that electron-withdrawing substituents close to the N-O function could stabilize spin adducts.^{9e,19}

Taking advantage of recent developments in the field,²⁰ in the present paper we also present DFT²¹ and MP2 calculations which were able to describe the EPR features of the novel spin

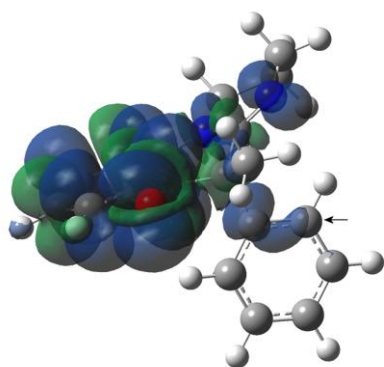


Figure 3: spin density distribution (α - β) of nitroxide **2a** computed at the B3LYP/EPR-III level (positive values in blue and negative in green). C-24 has been arrowed (see text).

This is in accordance with previous findings in other heteroaromatic analogues, such as indolinonic²⁵ and benzoxazinic nitroxides.²⁶ In line with this, the EPR spectra of nitroxides **2** were interpreted on the basis of hfcc typical of this kind of radicals, in which the nitrogen three lines are mainly split by two different couples of aromatic hydrogens of the heteroaromatic ring moiety (Figure 4), H(13) and H(15) with a larger hfcc (ca. 3 Gauss) and H(12) and H(14) with a smaller one (ca. 1 Gauss). In addition, the splitting of the amidine ring nitrogen N-21 was considered. The assignments, confirmed by means of appropriate DFT calculations previously described,²⁵ are reported in Table 2. However, because the experimental conditions followed in our study (aqueous medium in the presence of molecular oxygen) did not allow us to achieve a better spectral resolution than that shown in Figure 2, the hfcc values given in the last two columns of Table 2 are tentative and mainly based on DFT computational predictions.

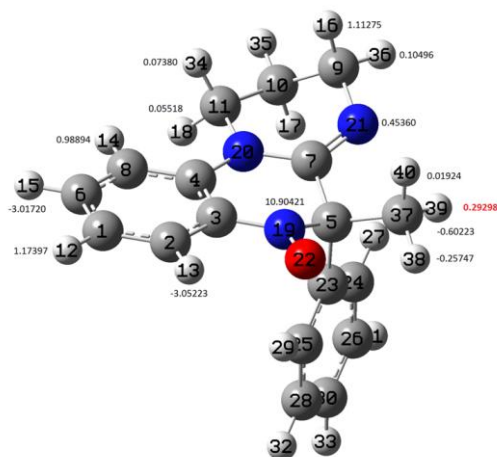


Figure 4: *Ball and stick* representation of the optimized geometry of nitroxide **2a** showing the arbitrary atom numbering and the corresponding hfcc computed at the B3LYP/EPR-III level.

Table 2. Experimental hyperfine coupling constants (in Gauss) of nitroxides **2** confirmed by computer simulation.

Nitroxide 2	N-19	H-13, 15	H-12, 14	N-21
a	10.77	3.13	0.88	0.29
b	10.84	3.12	0.89	0.23
c	10.76	3.08	0.88	0.31
d	10.64	3.07	0.91	0.41
e	10.62	3.09	0.98	0.57
f	10.53	3.08	0.87	0.47
g	10.55	3.04	0.83	0.67
h	10.90	3.15	0.80	0.24
i	10.45	3.48	0.89; 0.82 (N)	0.34

The isotropic hfcc (a_X) arises from the Fermi contact interaction between the unpaired electron and the nucleus (X), and is correlated to the corresponding spin density (ρ_X) by:

$$a_X = 2/3 \mu_0 g_e \mu_B g_X \rho_X$$

where μ_0 is the vacuum permeability, μ_B the Bohr magneton, g_e and g_X the electron and nuclear g -factor respectively.²⁷ The N-19 hfcc of spin adducts **2** (Table 2) decrease in the sequence: **h** > **b** > **a** > **c** > **d** > **e** > **g** > **f** > **i**, which can be ascribed to a decrease of the corresponding spin density in the same order. This is possibly due to the presence of an electron withdrawing group at C-24, the *ortho* position of the 5-aryl group, where a positive spin density has been found, as shown in Figure 3 for **2a**. At the same time, the fact that no significant spin densities have been found in any other position of such group explains why this effect upon N-19 is present only in aminoxyls **2e-g**. It should also be noted that derivatives **2e-g** may be subject to stereoelectronic effects due to the presence of the substituents in the *ortho*-position of the aromatic ring linked to the α -carbon. In **2i**, on the other hand, the decrease in the N-hfcc would be related to the electron withdrawing effect exerted by the presence of a conjugated nitrogen in position 8, also responsible of the large value found for the H-13,15 hfcc.

In order to evaluate the stability of the novel spin adducts, their EPR signals were followed by recording the corresponding spectra at different times until disappearance. Figure 5 shows the time-dependent EPR signal intensity of one of the new spin traps (compound **1d**) adduct.

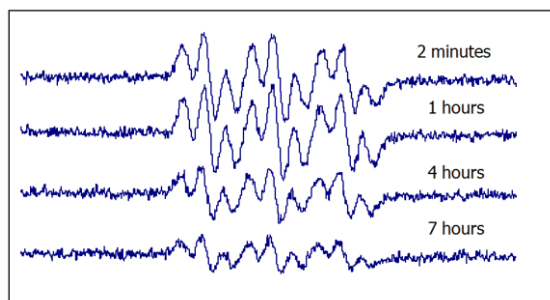


Figure 5. Time-dependent EPR spin adduct spectra of **1d** (10 mM final concentration) upon reaction with methyl radicals produced by a Fenton reaction. (1.33 mM FeSO₄ plus 3.33 mM H₂O₂, final concentrations) in PBS pH 7.6 containing 33% DMSO.

Comparatively, the DMPO/·CH₃ adduct was less stable as a function of time, as can be seen in Figure 6.

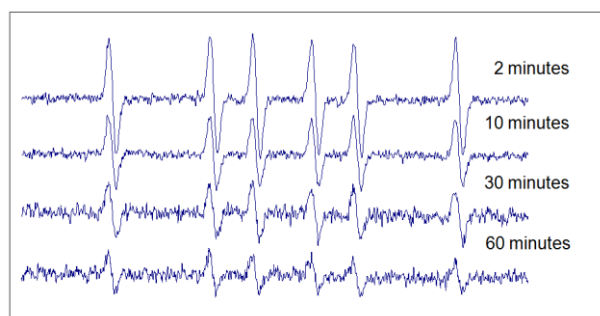


Figure 6. Time-dependent EPR spectra of DMPO/·CH₃ spin adduct. DMPO (10 mM final concentration) was tested in a Fenton reaction. (1.33 mM FeSO₄ plus 3.33 mM H₂O₂, final concentrations) in PBS pH 7.6 containing 33% DMSO.

To further investigate this difference, a competition experiment between DMPO and **1a** was performed, and EPR spectra are shown in Figure 7.

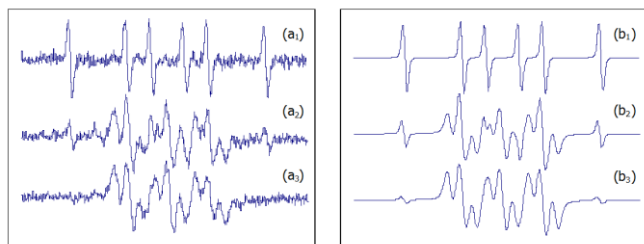


Figure 7. (a) Experimental and (b) simulated EPR spectra of the competition assay between DMPO and **1a** adducts. FeSO₄ (1.33 mM, final concentration) and H₂O₂ (3.33 mM, final concentration) were added to a solution containing both DMPO and compound **1a** in 33 % DMSO-PBS pH 7.6. Spectra a₁, a₂ and a₃ are the experimental EPR signals obtained at 1, 15 and

30 minutes and b₁, b₂ and b₃ are their respective simulated EPR spectra.

This experiment reveals the persistence of the signal of the novel adducts after DMPO adduct signal disappearance. Hence, even if the newly synthesized nitrones react more slowly with methyl radicals than DMPO, the corresponding adducts resulted much more persistent. The enhanced stability of adducts **2** would result from the absence of a hydrogen α - to the N-O· group, which is the main issue concerning the stability of DMPO spin adducts.¹⁸

The kinetics of formation and decomposition of the spin adducts generated by methyl radicals addition to the new nitrones **1** were then studied. The experimental conditions were modified to prevent precipitation of some derivatives and to enhance signal intensity, using a higher proportion of DMSO and H₂O₂ (see Experimental). Figure 8 shows the spin adduct formation and decomposition kinetics for amidinoquinoxaline *N*-oxide **1a** in the trapping-Fenton reaction system.

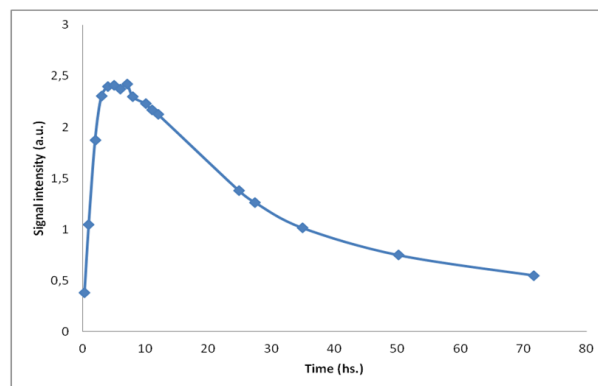


Figure 8. Spin adduct formation and decay kinetics of the spin trap **1a** in the Fenton reaction system.

Since the EPR signal recorded during the kinetic experiments was due exclusively to the aminoxyls under investigation, it was possible to use high modulation conditions to merge together all the small signal splittings; in such conditions the EPR signal was reduced to a broad triplet of triplets, which could be easily handled for kinetic measurements. The experimental addition rate constants are listed in Table 3.

Table 3: Experimental rate constants (k_{add} in sec^{-1}) corresponding to the addition reaction and selected nitrone **1** dihedral angle.

Compound 1	$k_{\text{add}} \cdot 10^4$	Dihedral angle (Figure 9) ($^\circ$)
a	2.559	-45.29
b	3.655	-41.33
c	3.947	-43.66
d	3.319	-44.86
e	0.486	-60.26
f	0.380	-66.31
g	0.311	-75.55
h	1.034	-43.38
i	0.521	-45.70

The rate of the addition is low, a fact that may be attributed to steric hindrance of the 5-aryl group, which is twisted with respect to the heterocyclic core in the ground state (Figure 9, Table 3).

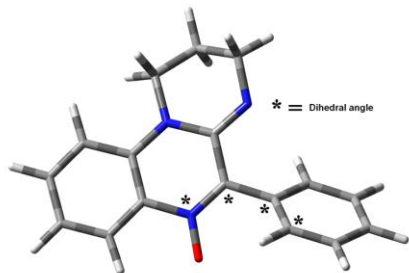


Figure 9. MPW1K/6-31G(d) Ground state geometry of nitrone **1a**.

The steric hindrance is more important for the *ortho* substituted derivatives **1e-g**, which have restricted rotation around the C5-Ar bond.¹⁶ The rate constants for this subgroup follow the order $\text{OCH}_3 > \text{Cl} > \text{I}$, which parallels the increasing Van der Waals radii of the *ortho* substituents. A plot of $-\ln k_{\text{add}}$ vs. steric parameters (Sternhell scale²⁸) shows an excellent linear correlation (Figure 10). The steric volume of the *ortho* substituent determines the dihedral angle between the Ar group and the heterocyclic core in the ground state (Table 3), which in turn influences the steric hindrance exerted by the 5-substituent.

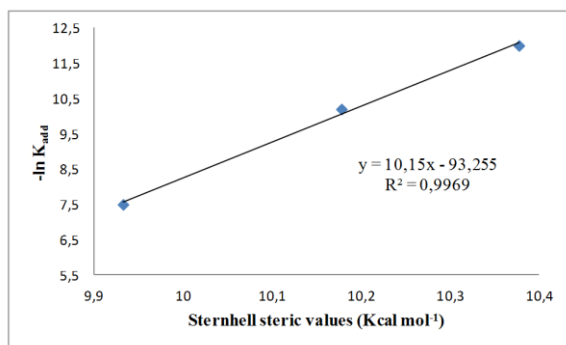


Figure 10: $-\ln k_{\text{add}}$ vs. Sternhell steric parameters

On the other hand, *para* substitution (compounds **1a-d**) does not induce significant changes in k_{add} , while modifications in the fused ring (compound **1i**) or in the nature of the 5-substituent (compound **1h**) bring about noticeable effects on the addition rates. In order to assess the importance of electronic effects on the addition rate constants, a NBA analysis was carried out at the MP2/6-31G(d) level to compute the corresponding atomic charges at the nitro α -carbon (Table 4).

Table 4. MP2/6-31G(d) computed C-5 atomic charges.

Compound 1	C5 MP2 charge
a	0.13710
b	0.13673
c	0.13554
d	0.13582
h	0.14087
i	0.14543

The plot of $-\ln k_{\text{add}}$ vs MP2 charges, reported in Figure 11, shows a clear dependence of the rate constant from atomic charge at the nitro α -carbon, according to literature reports.²⁹

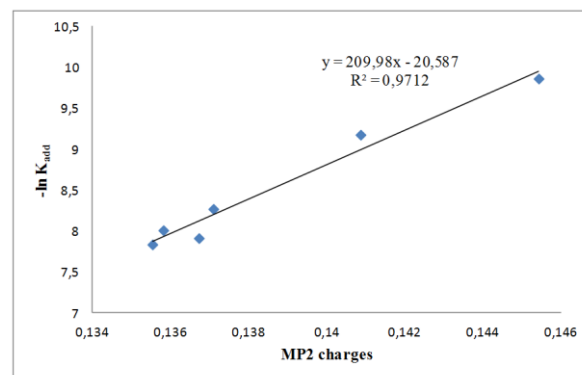


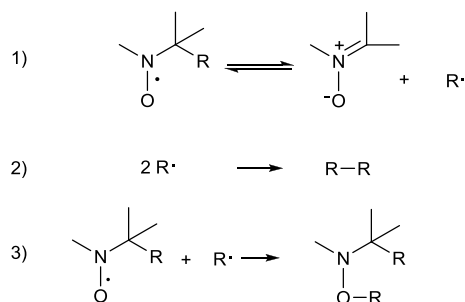
Figure 11. $-\ln k_{\text{add}}$ as a function of MP2 charge densities.

Spin adducts decomposition of all spin traps followed a pseudo-first order kinetics. Their respective k_{dec} and half-life times ($t_{1/2}$) are informed in Table 5.

Table 5. Decomposition rate constants and half-life times of nitroxides **2**.

Spin adduct 2	$k_{\text{dec}} \cdot 10^5 \text{ (s}^{-1}\text{)}$	$t_{1/2} \cdot 10^{-3} \text{ (s)}$
a	0.792	87.51
b	1.070	64.80
c	1.321	52.46
d	1.511	45.87
e	0.265	261.32
f	0.487	142.21
g	0.397	174.42
h	1.730	40.07
i	1.157	59.91

The overall spin adducts decomposition could be simplified as in the following scheme:



Scheme 2. Reactions involved in the spin adduct decomposition.

Assuming the reversibility of the first reaction, the C-centered radicals formed in this step can undergo self-coupling and/or react with the nitroxide in excess present in the reaction medium. Both these two last processes are extremely fast and largely shift the equilibrium of the first step to the right, also allowing to approximate the observed EPR signal decay to a pseudo first order process. The $t_{1/2}$ values reported in Table 5 have been determined following this assumption.

In spite of the previous considerations, other chemical reactions cannot be ruled out in the oxidative aqueous reaction medium. Therefore, no clear relationship between structure and decomposition rates of the spin adducts comprising all the compounds under study could be established. In spite of this, analysis of the results reported in Table 5 clearly show that *ortho* substitution stabilizes the spin adducts, as can be seen on comparing the decomposition rate constants of compounds **2e** and **2f** with the corresponding *para* isomers (**2b** and **2c**, respectively). An attempt to correlate the nitroxide decomposition rate constant with the corresponding dihedral angle has been reported in Figure 12:

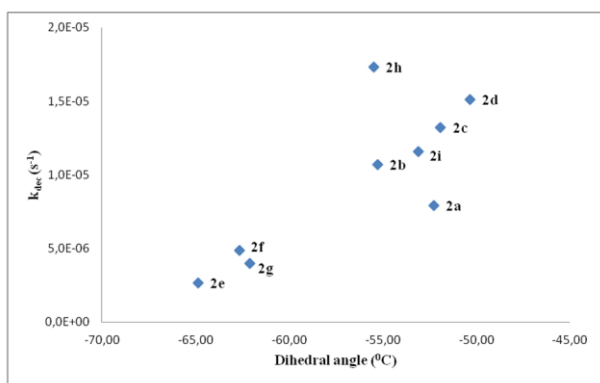


Figure 12. Decomposition rate constants (k_{dec} in sec^{-1}) of nitroxides **2** vs. the corresponding dihedral angle N19-C5-C23-C25 (in degrees) (see Figure 4).

Upon this basis, it could be hypothesized that the more “twisted” the nitrone, the more persistent is the corresponding spin adduct. This could be likely due to the fact that in nitroxides **2e-g** it becomes more difficult to reach the planarity necessary for the formation of

the nitrone N=C double bond required by the adduct decomposition process as shown in Figure 13, where the computed geometry of the Transition State for nitroxide **2a** decomposition has been reported as an example.

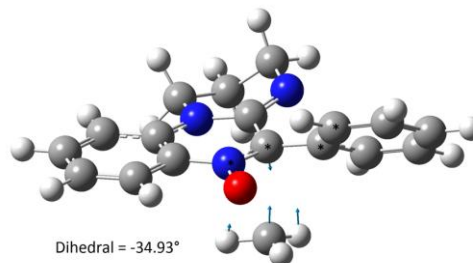


Figure 13. Decomposition Transition State geometry of aminoxyl **2a** computed at the MPW1K/6-31G(d) level.

Conclusions

We present in this work a novel type of spin traps derived from the pyrimidoquinoxaline *N*-oxide heterocyclic core. The structural variations comprise the steric and electronic features of the aryl substituent at the nitrone α -carbon and the nature of the fused aryl ring. EPR spin trapping technique showed that all the derivatives were able to trap methyl radicals generated in a Fenton reaction system in the presence of DMSO. The corresponding nitroxides were characterized by EPR and their hfcc were assigned on the basis of related heterocyclic systems and confirmed by DFT calculations. The values of the N-hfcc were indicative of extensive electron delocalization in the adducts due to the high level of coplanarity of the condensed rings within the amidinoquinoxaline system. As a consequence, the novel spin traps showed remarkably persistent signals, as evidenced in a competition experiment between derivative **1a** and DMPO.

The kinetics of formation and decomposition of the spin adducts were studied. In both processes, a clear dependence on *ortho* substitution at the 5-aryl group was identified as the main general trend. In fact, both rates of formation and decomposition are significantly lower in *ortho* substituted derivatives. For the decomposition rate constants, a clear dependence on structural features could not be established. On the other hand, very good correlations were found between steric and electronic parameters of the nitrones and their $\cdot\text{CH}_3$ addition rates. Taken together, these results represent an insight into the relevant structural features that influence the spin trapping efficiency of this novel type of nitrones, to be taken into account for the future design of new derivatives based on this heterocyclic scaffold.

Experimental

Synthesis

General

Melting points were determined with a Büchi capillary apparatus and are uncorrected. ^1H and ^{13}C NMR spectra were recorded on a Bruker Avance II 500 MHz spectrometer, using deuteriochloroform as the solvent. Chemical shifts are reported in parts per million (δ) relative to TMS as an internal standard. Coupling constants are reported in Hz. D_2O was employed to confirm exchangeable protons (ex). Splitting multiplicities are reported as singlet (s), broad signal (bs), doublet (d), double doublet (dd), doublet of double doublets (ddd), triplet (t), triple doublet (td), pentet (p), and multiplet (m). Elemental analyses were determined using an Exeter CE 440 elemental analyzer. Reagents, solvents, and starting materials were purchased from standard sources and purified according to literature procedures.

Synthesis of 5-aryl-2,3-dihydro-1H-pyrimido[1,2-a]quinoxaline 6-oxides 1. General procedure.

A mixture of the corresponding aminoamide (1 mmol) and ethyl polyphosphate (PPE, 1 mL/0.05 g) was refluxed for 5 h. After reaching room temperature, the resulting solution was extracted with water (5 x 6 mL). The aqueous phases were pooled, filtered and made alkaline with 10% aqueous NaOH. The mixture was extracted with chloroform (3 x 15 mL). The organic phases were washed with water, dried over sodium sulphate and filtered. The chloroformic solution was left at r.t. until no further conversion to compounds **1** was evidenced by TLC (silica gel, chloroform:methanol 9:1). The solvent was then removed in vacuo and the crude product was purified by column chromatography (silica gel, chloroform:methanol 10:0-9:1). Compounds **1a-d**,¹⁴ **1f**¹⁶ were described in the literature. Yields and analytical data of compounds **1e,g-i** are as follows.

5-(2-Methoxyphenyl)-2,3-dihydro-1H-pyrimido[1,2-a]quinoxaline 6-oxide (1e).

This compound was obtained as a yellow solid, (0.141 g, 46%), mp 191-193°C (from hexane/ethyl acetate). ^1H NMR (500 MHz, CDCl_3 , 25 °C, TMS): δ = 8.38 (1H, dd, J =8.2, 1.4), 7.51-7.54 (1H, m), 7.43 (1H, ddd, J =8.5, 7.5, 1.7), 7.30 (1H, dd, J =7.5, 1.7), 7.19 (1H, ddd, J =8.2, 7.3, 1.1), 7.12-7.14 (1H, m), 7.08 (1H, td, J =7.5, 0.9), 7.03 (1H, dd, J =8.5, 0.9), 3.92 (2H, t, J =6.2), 3.82 (3H, s), 3.56-3.69 (2H, m, bs), 3.41 (2H, s), 2.02-2.09 (2H, m). ^{13}C NMR (125 MHz, CDCl_3 , 25 °C): δ = 157.2, 145.4, 139.2, 135.0, 131.6, 131.0, 130.6, 130.4, 121.9, 121.2, 120.8, 119.1, 111.5, 111.2, 55.9, 44.0, 43.8, 19.5. Anal. Calcd for $\text{C}_{18}\text{H}_{17}\text{N}_3\text{O}_2$: C, 70.3; H, 5.6; N, 13.7. Found: C, 70.1; H, 5.8; N, 13.6%.

5-(2-Iodophenyl)-2,3-dihydro-1H-pyrimido[1,2-a]quinoxaline 6-oxide (1g).

This compound was obtained as a yellow solid, (0.206 g, 51%), mp 153-155 °C (from hexane/ethyl acetate). ^1H NMR (500 MHz, CDCl_3 , 25 °C, TMS): δ = 8.40 (1H, dd, J = 8.2, 1.4), 7.95 (1H, dd, J = 8.0, 0.9), 7.56 (1H, dd, J = 8.6, 7.1), 7.50-7.53 (1H,

m), 7.32 (1H, dd, J = 7.8, 1.4), 7.20 (1H, ddd, J = 8.2, 7.1, 1.0), 7.16-7.18 (1H, m), 7.13 (1H, dd, J = 8.6, 1.0), 3.93-3.98 (1H, m), 3.86-3.91 (1H, m), 3.62-3.68 (1H, m), 3.52-3.57 (1H, m), 2.05-2.11 (2H, m). ^{13}C NMR (125 MHz, CDCl_3 , 25 °C): δ = 144.43, 142.61, 139.01, 136.48, 135.36, 131.91, 130.53, 130.33, 130.01, 128.41, 121.69, 121.28, 110.99, 97.44, 44.49, 43.64, 19.58. Anal. Calcd for $\text{C}_{17}\text{H}_{14}\text{N}_3\text{O}$: C, 50.6; H, 3.5; N, 10.4. Found: C, 50.6; H, 3.7; N, 10.3%.

5-(3-Thienyl)-2,3-dihydro-1H-pyrimido[1,2-a]quinoxaline 6-oxide (1h).

This compound was obtained as a yellow solid (0.153 g, 54%), mp 160-161°C. (from hexane/chloroform). ^1H NMR (500 MHz, CDCl_3 , 25 °C, TMS): δ = 8.61 (1H, dd, J =3.1, 1.0), 8.40 (1H, dd, J =8.4, 1.3), 7.89 (1H, dd, J = 5.1, 1.0), 7.45-7.49 (1H, m), 7.30 (1H, dd, J = 5.1, 3.1), 7.15-7.18 (1H, m), 7.03 (1H, d, J = 8.5), 3.87 (2H, t, J = 6.2), 3.66 (2H, t, J = 5.5), 2.08 (2H, m). ^{13}C NMR (125 MHz, CDCl_3 , 25 °C): δ = 144.5, 136.2, 134.4, 132.6, 131.2, 130.2, 130.1, 128.6, 122.4, 121.7, 121.1, 110.5, 44.4, 43.9, 19.9. Anal. Calcd for $\text{C}_{15}\text{H}_{13}\text{N}_3\text{OS}$: C, 63.6; H, 4.6; N, 14.8. Found: C, 63.4; H, 4.7; N, 14.7%.

8H-Pyrido[3',2':5,6]pyrazino[1,2-a]pyrimidine-9,10-dihydro-6-phenyl 5-oxide (1i).

This compound was obtained as a yellow solid (0.142 g, 51%), mp 215-217°C. (from hexane/chloroform). ^1H NMR (500 MHz, CDCl_3 , 25 °C, TMS): δ = 8.55 (1H, dd, J = 8.0, 1.7), 8.42 (1H, dd, J = 4.8, 1.7), 7.59-7.62 (2H, m), 7.47-7.51 (2H, m), 7.42-7.46 (1H, m), 7.10 (1H, dd, J = 8.0, 4.8), 4.22 (2H, t, J = 6.2), 3.66 (2H, t, J = 5.6), 1.99-2.03 (2H, m). ^{13}C NMR (125 MHz, CDCl_3 , 25 °C): δ = 149.9, 145.3, 144.8, 141.2, 130.1, 129.6, 129.3, 129.1, 128.0, 126.2, 117.3, 45.7, 41.3, 19.6. Anal. Calcd for $\text{C}_{16}\text{H}_{14}\text{N}_4\text{O}$: C, 69.05; H, 5.1; N, 20.1. Found: C, 70.1; H, 5.2; N, 20.0%.

Spin adducts characterization and competition experiments

EPR spectra were recorded at 20°C using an X-band EPR Spectrometer Bruker ECS 106. General EPR spectrometer settings: center field 3480 Gauss; sweep width 80 Gauss; time constant 2.56 ms; conversion time 2.56 ms; modulation amplitude 0.1 Gauss; modulation frequency 50 kHz; receiver gain 2×10^4 ; microwave power 10 mW. EPR spectra simulations were carried out by means of the Winsim program, freely available from NIEHS.³⁰

Kinetic experiments

Each nitron (5mM final concentration) was tested in a Fenton reaction (0.72 mM FeSO_4 plus 147 mM H_2O_2 , final concentrations) in DMSO with 33% PBS (phosphate buffered saline) pH 7.6. Nitroxide radical signal was measured as the peak-to-peak intensity variation. Kinetic experiments were performed at least three times and rate constants were determined as averaged values from the independent runs. EPR spectra were recorded at 20°C using an X-band EPR Spectrometer Bruker EMX Plus. General EPR spectrometer settings: center field 3512 Gauss; sweep width: 100 Gauss; time

constant 5.12 ms; conversion time 5.12 ms; modulation amplitude: 0.75 G; modulation frequency 50 kHz, receiver gain 1×10^5 ; microwave power 10 mW. The spectra are the result of the accumulation of a variable number of scans in order to improve signal-to-noise ratio.

Computational Details

Density Functional Theory calculations²¹ were carried out using the GAUSSIAN 09 suite of programs³¹ on an EURORA EUROTECH Cluster at Cineca Supercomputing Center.³² All aminoxyls geometries were optimized at the B3-LYP/6-31G(d) level of theory and were carried out with the unrestricted formalism, giving $\langle S^2 \rangle = 0.7501 \pm 0.0003$ for spin contamination (after annihilation). Aminoxyls conformations were systematically screened by means of appropriate relaxed (i.e., with optimization at each point) Potential Energy Surface Scans to ensure that species were global minimum energy structures. In addition, in frequency calculations, imaginary (negative) values were never found, confirming that the computed geometries were always referred to a minimum. EPR parameters calculations were performed following the multistep procedure previously described.²⁵ Transition State optimizations were performed employing the MPWIK functional³³ in conjunction with the 6-31G(d) basis set for optimizations and 6-31+G(d,p) for frequency calculations; in these last runs, all optimized stationary points were found to have the appropriate number of imaginary frequencies, and the imaginary modes (negative sign) corresponded to the correct reaction coordinates, also confirmed by their visualization with appropriate programs.

Acknowledgements

This work was supported by the University of Buenos Aires (20020100100935) and by CONICET (PIP 286). MIUR (Ministero dell'Università e della Ricerca Scientifica e Tecnologica) is kindly acknowledged for financial support (2010PFLRJR - project PROxi) (P.S.) and Cineca Supercomputing Center for computational resource allocation (IS CRA grant ALKOXY-B, code: HP10CYGED5).

Notes and references

^a Departamento de Química Orgánica. Facultad de Farmacia y Bioquímica. Universidad de Buenos Aires. CONICET. Junín 956, (1113) Buenos Aires, Argentina.

^b Cátedra de Física. Departamento de Fisicomatemática. Facultad de Farmacia y Bioquímica. Universidad de Buenos Aires. Junín 956, (1113) Buenos Aires, Argentina.

^c S.I.M.A.U. Department - Chemistry Division, Università Politecnica delle Marche, via Breccia Bianche 12, I-60131 Ancona, Italy.

* Corresponding author: Tel./fax +5411 49648252 (L. R. O.). Email: lorelli@ffyba.uba.ar (L. R. O.), pstipa@univpm.it (P. S.).

Electronic Supplementary Information (ESI) available: Experimental details and spectral data for all the new compounds. See DOI: 00.0000/b0000000x/

- (a) A. Mackor, Th. A. J. W. Wajer and Th. J. de Boer, *Tetrahedron Lett.* 1966, **7**, 2115. (b) M. Iwamura and N. Inamoto, *Bull. Chem. Soc. Jpn.*, 1967, **40**, 702. (c) G. R. Chalfont, M. J. Perkins and A. Horsfield, *J. Am. Chem. Soc.*, 1968, **90**, 7141. (d) E. G. Janzen and B. J. Blackburn, *J. Am. Chem. Soc.*, 1968, **90**, 5909. (e) C. Lagerscrantz and S. Forshult, *Nature*, 1968, **218**, 1247.
- J. A. Berliner and J. W. Heinecke, *Free Radical Biol. Med.*, 1996, **20**, 707.
- (a) R. T. Dean, S. Fu, R. Stocker and M. J. Davies, *Biochem. J.*, 1997, **324**, 1; (b) S. Fu, M. J. Davies, R. Stocker, R. T. Dean, *Biochem. J.*, 1998, **333**, 519.
- (a) J. Moskovitz, M. B. Yim and P. B. Chock, *Arch. Biochem. Biophys.*, 2002, **397**, 354; (b) R. A. Floyd and K. Hensley, *Neurobiol. Aging*, 2002, **23**, 795.
- (a) E. G. Janzen, *Acc. Chem. Res.*, 1971, **4**, 31. (b) C. A. Evans, *Aldrichimica Acta*, 1979, **12**, 23. (c) C. Mottley and R. P. Mason, in *Biological Magnetic Resonance 8*, ed. L. J. Berliner, J. Reuben, Plenum Publishers, New York, 1989, p 489. (d) P. Tordo, *Electron Paramagn. Reson.* 1998, **16**, 116. (e) G. R. Buettner, *Free Radical Biol. Med.*, 1987, **3**, 259. (f) E. G. Janzen and J. I.-P. Liu, *J. Magn. Reson.*, 1973, **9**, 510. (g) E. G. Janzen, C. A. Evans and J. I.-P. Liu, *J. Magn. Reson.*, 1973, **9**, 513. (h) E. G. Janzen, in *Free Radicals in Biology*, ed. W. A. Prior, Academic Press, New York, 1980, p 115.
- C. Fréjaville, H. Karoui, B. Tuccio, F. Le Moigne, M. Culcasi, S. Pietri, R. Lauricella and P. Tordo, *J. Med. Chem.*, 1995, **38**, 258.
- Y. Kotake and E. G. Janzen, *J. Am. Chem. Soc.*, 1991, **113**, 9503.
- (a) K. Makino, T. Hagiwara, H. Imaishi, M. Nishi, S. Fuji, H. Ohya and A. Murakami, *Free Radical Res. Commun.*, 1990, **9**, 233. (b) E. Finkelstein, G. M. Rosen and E. J. Rauckman, *Mol. Pharmacol.*, 1982, **21**, 262.
- (a) R. D. Hinton and E. G. Janzen, *J. Org. Chem.*, 1992, **57**, 2646. (b) A. Zeghdoui, B. Tuccio, J.-P. Finet, V. Cerri and P. Tordo, *J. Chem. Soc., Perkin Trans. 1*, 1995, 2087. (c) E. G. Janzen, Y.-K. Zhang and D. L. Haire, *Magn. Reson. Chem.*, 1994, **32**, 711. (d) C. Fréjaville, H. Karoui, B. Tuccio, F. Le Moigne, M. Culcasi, S. Pietri, R. Lauricella and P. Tordo, *J. Chem. Soc., Chem. Commun.*, 1994, 1793. (e) C. Fréjaville, H. Karoui, B. Tuccio, F. Le Moigne, M. Culcasi, S. Pietri, R. Lauricella and P. Tordo, *J. Med. Chem.*, 1995, **38**, 258. (f) K. Stolze, N. Udilova and H. Nohl, *Biol. Chem.*, 2002, **383**, 813. (g) K. Stolze, N. Udilova, T. Rosenau, A. Hofinger and H. Nohl, *Biol. Chem.*, 2003, **384**, 493. (h) H. Zhao, J. Joseph, H. Zhang, H. Karoui and B. Kalyanaraman, *Free Radical Biol. Med.*, 2001, **31**, 599. (i) G. Olive, A. Mercier, F. Le Moigne, A. Rockenbauer and P. Tordo, *Free Radical Biol. Med.*, 2000, **28**, 403.
- (a) P. Tsai, S. Pou, R. Straus and G. M. Rosen, *J. Chem. Soc., Perkin Trans. 2*, 1999, 1759. (b) G. M. Rosen, P. Tsai, E. D. Barth, G. Dorey, P. Casara, M. Spedding and H. J. Halpern, *J. Org. Chem.*, 2000, **65**, 4460; P. Astolfi, M. Marini and P. Stipa, *J. Org. Chem.* 2007, **72**, 8677.
- G. E. Adams, E. M. Fielden, M. A. Naylor and I. J. Stratford, *UK Pat. Appl. GB 2257360*, 1993.

- 12 P. C. Parthasarathy, B. S. Joshi, M. R. Chaphekar, D. H. Gawad, L. Anandan, M. A. Likhate, M. Hendi, S. Mudaliar, S. Iyer, D. K. Ray and V. B. Srivastava, *Indian J. Chem. Sect. B*, 1983, **22**, 1250.
- 13 G. J. Ellames, K. R. Lawson, A. A. Jaxa-Chamiec and R. M. Upton, *EP* 0256545, 1988.
- 14 M. B. García, L. R. Orelli, M. L. Magri and I. A. Perillo, *Synthesis*, 2002, 2687.
- 15 M. B. García, L. R. Orelli and I. A. Perillo, *J. Heterocycl. Chem.*, 2006, **43**, 1703.
- 16 J. E. Díaz, M. B. García and L. R. Orelli, *J. Mol. Struct.*, 2010, **982**, 50.
- 17 M. L. Lavaggi, G. Aguirre, L. Boiani, L. Orelli, B. García, H. Cerecetto and M. González, *Eur. J. Med. Chem.*, 2008, **43**, 1737.
- 18 (a) R.-M. Dupeyre and A. Rassat, *J. Am. Chem. Soc.*, 1966, **88**, 3180. (b) K. Adamic, D. F. Bowman, T. Gillan and K. U. Ingold, *J. Am. Chem. Soc.*, 1971, **93**, 902.
- 19 (a) H. Karoui, C. Nsanzumuhire, F. Le Moigne and P. Tordo, *J. Org. Chem.*, 1999, **64**, 1471. (b) A. Allouch, V. Roubaud, R. Lauricella, J.-C. Bouteiller and B. Tuccio, *Org. Biomol. Chem.*, 2005, **3**, 2458.
- 20 For a review see R. Improta and V. Barone, *Chem. Rev.*, 2004, **104**, 1231.
- 21 (a) R. G. Parr and W. Yang, in *Density Functional Theory of Atoms and Molecules*, Oxford University Press, New York, NY, 1998; (b) W. Koch and M. C. A. Holthausen, in *Chemist's Guide to Density Functional Theory*, Wiley-VCH, Weinheim, Germany, 2000.
- 22 M. K. Eberhardt and R. Colina, *J. Org. Chem.* 1988, **53**, 1071.
- 23 (a) A. Di Matteo, C. Adamo, M. Cossi, V. Barone and P. Rey, *Chem. Phys. Lett.*, 1999, **310**, 159. (b) A. Di Matteo, C. Adamo, V. Barone and P. Rey, *J. Phys. Chem.*, 1999, **103**, 3481. (c) A. Di Matteo, A. Bencini, M. Cossi, V. Barone, M. Mattesini and F. Totti, *J. Am. Chem. Soc.*, 1998, **120**, 7069. (d) V. Barone, A. Grand, D. Luneau, P. Rey, C. Minichino and R. Subra, *New J. Chem.*, 1993, **17**, 545. (e) J. Cirujeda, J. Vidal-Gancedo, O. Jürgens, F. Mota, J. J. Novoa, C. Rovira and J. Veciana, *J. Am. Chem. Soc.*, 2000, **122**, 11393. (f) A. Zheludev, V. Barone, M. Bonnet, B. Delley, A. Grand, E. Ressouche, P. Rey, R. Subra and J. Schweizer, *J. Am. Chem. Soc.*, 1994, **116**, 2019. (g) S. M. Mattar and A. L. Stephens, *Chem. Phys. Lett.*, 2000, **319**, 601.
- 24 A. Alberti, in *Nitroxide Radicals and Nitroxide Based High-Spin Systems*, *Landolt-Börnstein – Group II Molecules and Radicals*, 2005, **26D**, pp. 1-6.
- 25 P. Stipa, *Chem. Phys.*, 2006, **323**, 501.
- 26 P. Astolfi and P. Stipa, *J. Org. Chem.*, 2011, **76**, 9253.
- 27 W. Weltner, in *Magnetic Atoms and Molecules*, Dover, New York, 1989.
- 28 G. Bott, L. D. Field and S. Sternhell, *J. Am. Chem. Soc.*, 1980, **102**, 5618.
- 29 F. A. Villamena, C. M. Hadad and J. L. Zweier, *J. Am. Chem. Soc.*, 2004, **126**, 1816.
- 30 D. Duling, *PEST Winsim*, version 0.96; National Institute of Environmental Health Sciences: Triangle Park, NC, 1996.
- 31 M. J. Frisch, *et al.*, Gaussian 09, Revision D.01.
- 32 Cineca Supercomputing Center, via Magnanelli 6/3, I-40033 Casalecchio di Reno, Bologna, Italy; <http://www.cineca.it/HPSystems>.
- 33 B. J. Lynch, P. L. Fast, M. Harris and D. G. Truhlar, *J. Phys. Chem. A*, 2000, **104**, 481.